

énergétique a été calculé suivant 2 hypothèses (sans expansion ou avec) (Tenerio-Tagle, 1988, ARAA 26, 150) quoiqu'il soit plus réaliste de penser que ces bulles soient plus jeunes et encore en expansion. Dans ce dernier cas nous avons supposé une vitesse d'expansion de 20 km/s ce qui est typique pour de tels objets. Les valeurs d'énergie obtenues sont réalistes, de l'ordre de 10^{52} erg. Pour ces objets il sera très intéressant d'étudier les champs de vitesse car ils sont très susceptibles d'indiquer une expansion.

En conclusion, la morphologie de plusieurs régions HII dans NGC 628 tend à démontrer que le milieu interstellaire est très inhomogène formé de bulles et filaments probablement du à l'action des vents stellaires d'étoiles jeunes et lumineuses. Ceci confirme plusieurs découvertes d'objets similaires dans la Voie Lactée et les galaxies du groupe local, quoiqu'à notre connaissance ce soit la première fois qu'on identifie des bulles dans une galaxie aussi éloignée que NGC 628.

*R. Arsenault, TCFH
J. Belley, et J.-R. Roy, Université Laval*

Deep High Resolution Galaxy Observations with an Infrared Array on CFHT

We recently had a very successful run on CFHT with a new Infrared Camera developed at the University of Hawaii. This instrument has been implemented by Klaus Hodapp and John Rayner at the Institute for Astronomy. It employs a 256x256 HgCdTe array manufactured by Rockwell as part of the NICMOS program (a 2nd generation instrument for HST). The array has 40 micron pixels which, with 1-to-1 re-imaging optics gives a plate scale of $0.29''/\text{pix}$ at CFHT's Cass focus. As well as its impressively large format, the array is characterized by low read-noise and dark-current. Together these make it an instrument whose operation from the astronomer's perspective, is remarkably similar to that of an optical CCD camera.

The normal method of observation for deep infrared imaging is to take a large number of individual exposures between which the telescope is moved in a mosaic pattern, ideally keeping the target object within the field of view of the array. Analysis of sequences of these independent images using conventional median sky-flattening techniques then allows the construction of a flat-field or background image as appropriate. If a windowing function is used through the sequence of images, then a time-varying background image can be generated. After sky-subtraction and flattening, the images are then co-registered and co-added. Experience with extremely long observations with the InSb arrays on UKIRT has been that flat-fielding of the final image to a few parts in 105 is possible.

In broad-band applications in J, H and K, the low noise characteristics of the new HgCdTe array means that the images are background-limited in less than one minute. This in turn allows the rapid acquisition of the independent images that go into the flat-field determination and, consequently, a more precise tracking of the flat-field pattern over time is possible. The wide field of view and small-pixel scale, coupled with CFHT's good seeing, also means that the coregistration of images, frequently a problem with small arrays in cases where the target object may not be visible on individual short exposure frames, is straightforward. There are almost always several field stars

visible on every image. The wide field of view allows relatively large steps in the mosaic pattern. This has the distinct advantage of reducing the effect of subtle negative ghosting of images introduced by the median flat-fielding process, since these are displaced much further from each object. We have found this aspect to be especially important in our work to determine the surface brightness profiles of very distant galaxies.

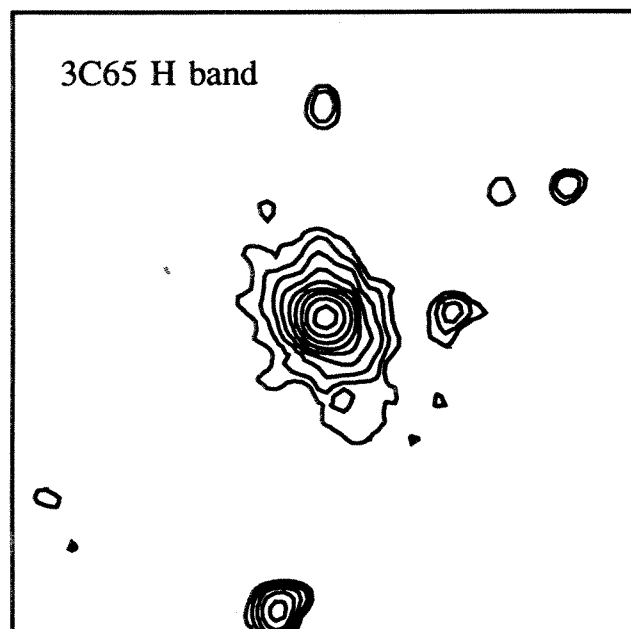


Figure 14: H-band (1.65 micron) image of 3C65 at $z = 1.175$. Total exposure was 74 minutes, integrated seeing is $0.75''$ FWHM. The image is $15''$ each side.

Despite conditions of intermittent fog and high humidity, we experienced conditions of good seeing during our run. As an example of the quality of our data, Figure 14 shows a 74-minute H-band image of the radio galaxy 3C65 ($z = 1.175$) obtained by coadding 37 individual 2-minute exposures. Even after the coregistration process the FWHM of this image is less than $0.75''$ and many of the individual images had $0.5''$ stellar images. The S/N in the central pixel close over 50, and the envelope of the galaxy may be traced out to beyond a radius of $4''$ (roughly 40 kpc for $H_0 = 50 \text{ km s}^{-1} \text{ Mpc}^{-1}$). The only frustration encountered in making these observations at CFHT was the necessity to stop auto-guiding at the end of each exposure, move the telescope to a new mosaic position, reacquire the guide star, restart auto-guiding and start a new exposure — to be repeated every 1-2 minutes. Telescopes such as UKIRT where this mode of observation is now commonplace have implemented schemes whereby these steps are automatically controlled by the camera itself. A similar set-up would be highly desirable at CFHT in the future, particularly when a facility infrared camera is available.

The image of 3C65 was obtained as part of a scientific program to study the morphology at near-infrared wavelengths of radio galaxies at high redshifts (i.e. at rest-wavelengths in the red-visual). The small dispersion and smooth continuity seen in the infrared K-z relation for radio galaxies out to redshifts $z = 2$ and beyond (despite a wide variation in optical-infrared color) argues that the infrared light is dominated by the light from an underlying massive gE-like galaxy. Such a conclusion has important consequences for our understanding of how and when massive galaxies form in the early Universe.

In this picture, the rest-frame ultraviolet emission seen at optical wavelengths comes from an "active" component of varying strength across the sample. Studies of the optical morphologies of these objects, including high resolution imaging by Hammer and Le Fèvre at CFHT, have revealed bizarre structures not encountered at low redshifts. The emission is frequently aligned along the axis of the radio source in blobs and elongated components. It is not yet known whether it is due to star-formation induced by the radio jet or whether it has a non-stellar origin. Regardless, this active component must be intimately associated with the active nucleus.

The present program was undertaken to study the infrared morphologies of high redshift radio galaxies to test the idea that the infrared light is dominated by a mature underlying galaxy, and if indeed it is, to then study this cosmologically important component. The results from the first phase of this project (to study a well-defined sample at $0.8 < z < 1.3$, mostly carried out on other telescopes but including our CFHT image of 3C65) has recently been submitted for publication. We find that, while the infrared images are in most cases still "aligned" with the radio source axis, this is a much weaker effect than that seen at optical wavelengths and is consistent with being produced by the long-wavelength "tail" of a roughly flat-spectrum active component underneath a much redder and symmetric "old-galaxy" component. Quantitative measures of the alignment indicate that typically only 10-20% of the infrared light can come from a component with the same morphological characteristics as the short wavelength ultraviolet light, with the remainder coming from a symmetric component.

In this context, 3C65 is especially interesting. It is the reddest radio galaxy known at these redshifts, and therefore presumably has least contamination from the active component associated with the nuclear activity. The high resolution and

depth of this image allows us to compare the scale size of this image with similar radio galaxies at lower redshifts. In Figure 15, we show the H-band surface brightness profile of 3C65. This follows a de Vaucouleur's $r^{1/4}$ law over a wide dynamic range. The derived effective radius (uncorrected for the effects of seeing) is $r_e = 1.0''$ or approximately 8.5 kpc for $q_0 = 0.5$. This value is close to the middle of the range of values of r_e found in low redshift radio galaxies.

Simon Lilly and Michael Rigler
Institute for Astronomy, University of Hawaii

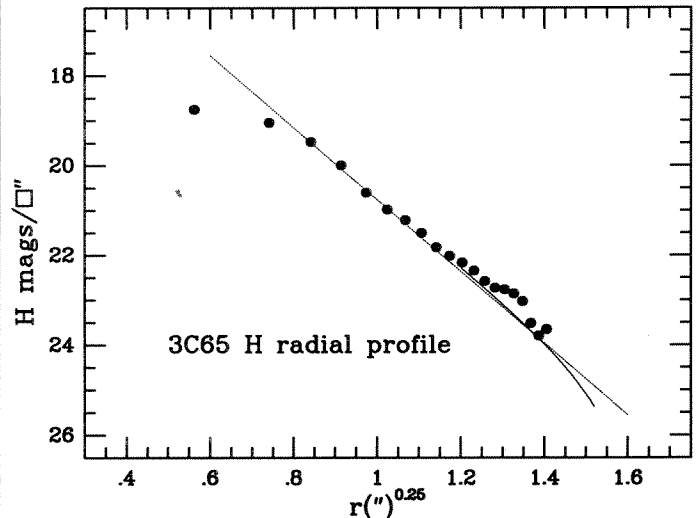


Figure 15: Surface brightness profile of 3C65 in the H-band, showing the reasonable fit to a de Vaucouleur's profile. Points represent observed surface brightness in annuli, curve represents a polynomial profile fitted to the outer regions of the galaxy. Dashed line indicates a de Vaucouleur's profile with $r_e = 1.0''$ (8.6 kpc).

High Resolution Imaging of the Young Star DD Tauri

In the last 5 years, evidence has accumulated for the existence of circumstellar disks around young stars. With a typical radius of 100 AU, these optically thick, presumably protoplanetary disks cover only a fraction of an arcsec on the sky, even at the distance of the nearest stellar formation regions (e.g., Taurus, $d=150\text{pc}$). High-resolution imaging techniques are therefore required to directly detect them.

With this goal in mind, we started a long-term program at CFHT dedicated to optical and near-IR high-resolution imaging of T Tauri stars, a class of very active, low-mass pre-main sequence stars. We report here preliminary results obtained on DD Tauri, which we found to possibly be surrounded by a circumstellar disk seen at high inclination.

Figure 16a shows contours from the first high-resolution image of DD Tau we obtained in October 1990 using the DAO High Resolution Camera at the telescope prime focus. The image was taken through a narrow-band filter ($\Delta\lambda=100\text{\AA}$) centered on $H\alpha$ with an exposure time of 10 seconds.

The object appears clearly resolved with two intensity peaks separated by $0.55 \pm 0.05''$ at P.A. = $186 \pm 3^\circ$. A narrow-band image centered on the continuum next to $H\alpha$ was kindly obtained a few days later by O. Le Fèvre with FOCAM and

confirmed the N-S elongation of the object, though the seeing was not good enough to clearly resolve it.

These results prompted us to perform near-IR speckle observations of DD Tau during our December 1990 run using the Observatoire de Paris-INSU CIRCUS IR camera. Under good seeing conditions, 600 images of DD Tau were obtained in the L' band ($3.8\mu\text{m}$) using a $0.1''/\text{pixel}$ spatial sampling and a 700ms exposure time. The individual images were recentered on the brightest pixel and co-added to yield the reconstructed image shown in Figure 16b, while the 2D visibilities are shown in Figure 16c.

The visibilities, i.e., the modulus of the 2D Fourier transform of the object, indicate a cut-off frequency of 3 arcsec^{-1} and exhibit a clear ripple pattern characteristic of binary stars. The object is thus well resolved at L with a separation of $0.53 \pm 0.05''$ at P.A. = $183 \pm 3^\circ$, a result consistent with that found from optical images.

The most straightforward interpretation of the high-resolution images is to assume that DD Tau is a binary, an already interesting result in itself since only a handful of sub-arcsecond pre-main sequence binaries have been detected to date. Alternatively, the two intensity peaks might correspond to stellar photons scattered above and below the plane of a circumstellar disk seen nearly edge-on. Little direct starlight would then reach the observer due to high obscuration by the optically thick disk.

Support to the disk interpretation is provided by the unusual forbidden lines profiles of DD Tau. Active pre-main sequence